

Gamma Spectroscopy with Germanium Detectors

Tyler Takaro

Cornell University Undergraduate
University of Washington REU Student

(Dated: August 21, 2015)

A large part of any rare event search is the minimization of backgrounds. To that end, this project aims to specify the activity of many commonly used pieces of electronic hardware, in order that future experiments may be done with a better knowledge of background contributions.

I. BACKGROUND

A. MAJORANA Collaboration

The MAJORANA collaboration[1] aims to detect neutrino-less double beta decay ($0\nu\beta\beta$) in ^{76}Ge , using an array of germanium p-type point contact detectors. An important factor in this effort is the minimization of backgrounds from any hardware which is needed to operate the detectors. In order to best understand and minimize this background, one must analyze the gamma spectrum from these pieces of hardware.

B. C1 Germanium Detector

C1 is a Reverse Electrode coaxial Germanium (REGe) detector manufactured by Canberra Industries owned by the Center for Experimental Nuclear Physics and Astronomy (CENPA) at the University of Washington. Though it originally had excellent energy resolution as a germanium detector, years of radiation damage have greatly hurt this resolution, as the full width at half maximum at 1.3 MeV has gone from a manufacture reported 2.6 keV to a measured 5.8 keV. This radiation damage has seemingly also hurt the efficiency of the detector, or the ratio of detected events to actual events, though this has been harder to quantify.

C1 measures the secondary γ rays emitted during β^- decay. The γ rays penetrate the detector, generating ionization via Compton scattering, promoting electron-hole pairs to their respective Compton bands in the semiconducting germanium. As the detector is biased at 5000 volts, the electrons follow the electric field, moving to the p+ contact, while the holes drift to the n+ contact. This induces an electrical current which is amplified and measured by the attached SIS3302 digitizer card. The card uses a trapezoidal filter which traces over the signal of each γ to determine a height of the signal. This recorded height is proportional to the energy of the γ detected.

In order to use C1, the proportionality of pulse height to energy must be calibrated. The detector was calibrated using a ^{40}K sample, as well as the ^{214}Bi and ^{208}Tl lines at 1764.5 keV and 2614.5 keV respectively, present in the background. In addition, the trapezoidal energy filter's gap and peaking times were adjusted to minimize

the energy resolution at 1460.8 keV, again using a ^{40}K sample.

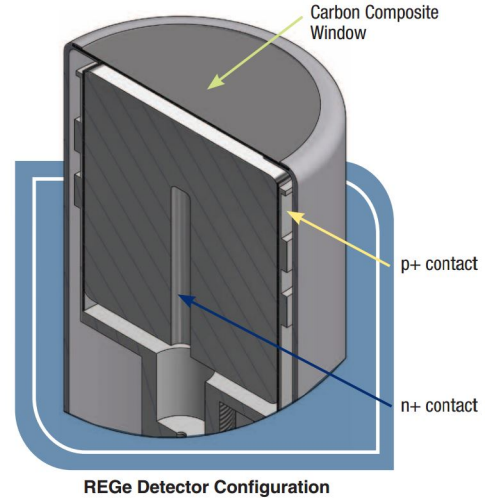


FIG. 1. A diagram of the C1 detector[2]

II. DATA TAKING METHODS

A. Converting Decays to Activity

In determining the activity of a sample from a measured number of decays, one must consider the time for which the sample is counted (here denoted as t), the mass of the sample (m), the efficiency of the detector (ϵ), and the branching ratio (b). The branching ratio describes how likely a given γ is to be generated by the decay of an isotope. These combine in the following way:

$$R = \frac{K}{tmeb} \quad (1)$$

This gives the activity R in units of Becquerel per kilogram.

B. Shielding

Our everyday environment is filled with γ radiation from natural radioactivity. For this reason, in order to

detect samples with relatively low radioactivity, radiation shielding must be used. Initially, a single layer of lead bricks was used, giving a shield thickness of 4 inches. This resulted in a reduction of the overall rate of events of roughly 90%.

After attempting to test the activity of a number of electronic components, only to realize that the sensitivity of the detector setup was too low, the radiation shielding was rebuilt with a second layer of lead. This meant a shield thickness of between 4 and 8 inches, depending on the angle of incidence of the γ particle. It also meant that any cracks between bricks were covered by other bricks, preventing any γ originating outside the shielding from having an uninterrupted line of sight to the detector. This further decreased the overall rate of events by approximately 25%, and decreased the rate of events in the region of interest (ROI) for uranium, thorium, and potassium of 50%.

After analyzing the background with the improved shielding configuration, it was found that the primary background contributions were from ^{110}Ag , and from ^{124}Sb . As lead is sometimes alloyed with silver, tin, and antimony, which could be turned into these unstable isotopes by neutron capture, it seemed that there were some neutron irradiated lead alloy bricks in the shield. This seemed especially plausible given the prevalence of experiments using high levels of neutron radiation ongoing in CENPA. After replacing seven of the innermost bricks with “clean” lead bricks, the background from ^{110}Ag was reduced by 50%, and from ^{124}Sb by 88%. However, the rate in the ROI for uranium, thorium, and potassium was unchanged by the new shielding, as expected.

C. Efficiency Calculation

In order to determine the actual activity of a sample, it is important to know the efficiency of the detector as accurately as possible. The absolute efficiency can be split up into a geometric factor and an intrinsic factor. The geometric factor represents the fractional solid angle area of the detector relative to the sample location. The intrinsic factor is due to the properties of the detector itself, and includes factors like the tendency for a particle to pass through the detector without reacting. To characterize the absolute efficiency, a variety of samples with known activities were tested with C1. Samples of ^{249}Cf , ^{137}Cs , ^{60}Co , and ^{40}K with γ emissions at 333 keV, 388 keV, 662 keV, 1173 keV, 1332 keV, and 1461 keV were used, and a linear fit was performed to the measured rates to approximate the energy dependence of the efficiency. See FIG 2. for the resulting efficiency function.

The error-bars for this calculation were calculated by first determining what fraction of the efficiency was due to the geometric factor. Once this was known, an uncertainty of the placement of the sample of ± 5 inches in any direction. This error was then propagated through the geometric calculation to give error bars on the efficiency.

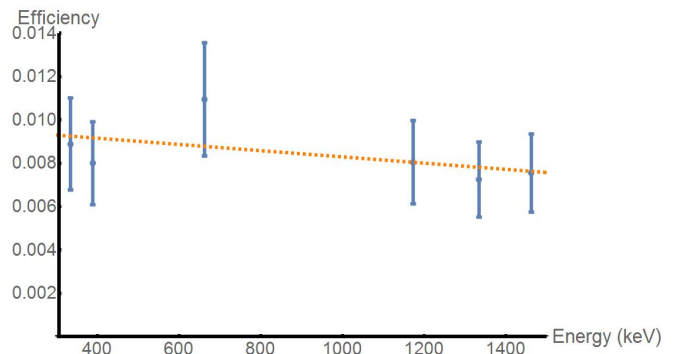


FIG. 2. The Efficiency of C1 as a function of energy.

D. Confidence Intervals

Given that gamma spectroscopy has an uncertainty governed by counting statistics, it is more useful to put an confidence interval on the activity of a sample than to merely give the measured activity. Ordinarily, one could merely use Gaussian statistics, to give a 90% confidence interval on a measured N events of $[N - 1.65\sqrt{N}, N + 1.65\sqrt{N}]$. However, when one has a physical limit, such as the fact that a sample cannot undergo less than 0 β decays during a time period, these confidence intervals fail if one end of the confidence interval crosses the physical limit. To deal with situations like this, Feldman and Cousins [3] determined a new way to create confidence intervals near physical limits.

All confidence listed hereafter apply for 90% confidence, and use the approach outlined in the Feldman and Cousins paper when near the physical limit

E. Self-shielding Sources

If a sample has a high density and/or a large volume, its measured activity will be lower than its actual activity by a non-trivial amount due to self-shielding of the sample. In order to get an accurate measurement of the activity for large samples, shielding was assumed to take on an exponential form:

$$\frac{I}{I_0} = e^{-\mu x} \quad (2)$$

where I is the measured intensity of radiation, I_0 is the output intensity, μ is the linear attenuation coefficient, and x is the distance through the attenuating material. The linear attenuation coefficient varies by material and γ energy, and published values are available online [4].

To determine this actual activity given a measured activity for a self-shielding source, the measured activity was calculated for the source with no shielding, then compared to the activity for the above exponential shielding.

$$I = \int_0^L \frac{K}{L} dx = K \quad (3)$$

$$I_0 = \int_0^L \frac{K}{L} e^{-\mu x} dx = \frac{K}{\mu L} (1 - e^{-\mu L}) \quad (4)$$

$$I_0 = \frac{I\mu L}{1 - e^{-\mu L}} \quad (5)$$

Note that this modeling of the self-shielding is a slight underestimate, as it assumes one-dimensional shielding, rather than shielding in three-dimensions.

III. CHALLENGES

A. ORCA Crashes

The first and perhaps most important challenge faced during the experiment was in using the data acquisition (DAQ) software ORCA. Roughly two weeks into the experiment, ORCA began to crash during data taking runs, seemingly with no discernible pattern, with some runs lasting only seconds while others ran smoothly for several hours before crashing.

In order to continue the experiment, a script was written in the ORCA scripting language to identify data taking run crashes, then take the necessary steps to restart the run without requiring user input. This was an effective workaround, as it allowed the experimenter to pull only the runs of requisite length, and discard the rest. However, it still resulted in a significantly lower amount of live-time for the experiment.

The software crashes were eventually solved by updating the operating system, uninstalling and reinstalling the software, and redoing the network connection between the detector and the DAQ computer.

B. Fiesta Ware Plate

One of the first samples tested was a Fiesta Ware plate manufactured before World War II. This plate made an excellent sample, as its glaze contained roughly 4.5 g of natural uranium. Given the natural uranium, one would expect the entire ^{238}U decay chain to be in equilibrium. However, it was found that an emission line from ^{234m}Pa , which occurs in .8% of ^{238}U decays was more prominent than an emission line from ^{214}Bi , which occurs in 15.3% of ^{238}U decays if the chain is in secular equilibrium. This indicated that the ^{238}U decay chain was not in equilibrium as had been expected.

Eventually it was surmised that in the production of the uranium glaze, the decay products must have been removed. This would have given the uranium at most 80 years to decay, which, given the 245,000 year half-life of ^{234}U , would not have allowed the ^{238}U decay chain to equilibrate. This theory matched well with the measured rates of ^{234m}Pa and ^{214}Bi .

C. Tungsten Brick

In measuring a block of what was originally thought to be depleted uranium, two problems arose. First, the block seemed to have a surprisingly low activity of ^{238}U -chain isotopes. The ^{214}Bi lines were smaller than the lines in the thorium decay chain, and the ^{234m}Pa line was nowhere to be found, seemingly contradicting the analysis of the Fiesta Ware. Together these indicated only a small amount of uranium in the sample, present as a natural impurity. This discovery, along with the high density of the sample, allowed the determination that the sample was actually tungsten.

The other problem was discovered in the measurement of the ^{232}Th decay chain. The chain was measured with the decay of three ^{232}Th daughters. ^{212}Bi was measured using the ^{208}Tl line at 2615 keV, ^{214}Pb was measured at 239 keV, and ^{228}Ac was measured at 911 keV, 965 keV, and 969 keV. Each of these seemingly should have been measured in equilibrium, but they were measured as follows:

Peak	Activity (Bq/kg)
^{212}Bi (2615 keV)	[2.617, 2.939]
^{214}Pb (239 keV)	[9.923, 13.167]
^{228}Ac (911 keV)	[3.866, 4.401]
^{228}Ac (965 & 969 keV)	[4.611, 5.311]

The higher than expected ^{228}Ac could be explained by double neutron capture from ^{226}Ra from the ^{238}U decay chain, however, an explanation for the overly high ^{214}Pb was not as easily discovered. The high rate calculation was mostly due to the high theoretical shielding for lower energy γ , but this should have corrected to the same level as the ^{208}Tl .

IV. SAMPLE ASSAY

A number of different samples were measured, mostly chosen for what they might tell us about the background radiation from hardware for gamma spectroscopy experiments. These samples were measured for their impurities in ^{238}U , ^{232}Th , and ^{40}K , by testing the γ lines at 1765 keV, 2615 keV, and 1641 keV respectively. The samples are listed below.

1. Ceramic disk capacitors: These were chosen to give an upper bound on the activity one might expect from typical electronic components. As they're made of ceramic, they have a high level of impurities.
2. Circuitboard from KATRIN: This was likewise chosen as a typical electronic component which one might use in an experiment. KATRIN is another collaboration which has a presence at the University of Washington, who was kind enough to let us borrow this old circuitboard to use as a sample.

3. Connectors containing beryllium copper: These electronic connectors were formerly used in the MAJORANA experiment, before they were determined to have too high of a background rate to be used. These are typical connectors which one might use for a high precision electronic experiment.
4. Block of beryllium copper: This sample of beryllium copper was used to get a better upperbound on the actual activity of the connectors containing beryllium copper, as it has significantly more mass than the connectors. However, due to the extensive shielding of the background, this measurement is likely not as precise as it could be.
5. Tungsten Brick: This sample was chosen because

Tungsten is a metal commonly used as a radiation shielding, so it useful to know its precise background contribution.

6. OFHC copper support: This support is used by the MAJORANA collaboration, as is indicative of the typical activity of clean copper.
7. Gasket flanges: These are typically used in securing a vacuum system. They're not made to be particularly clean, so they may have a high level of impurities.

The confidence intervals for the activities of each sample are listed in the following table:

Sample	^{238}U Activity (Bq/kg)	^{232}Th Activity (Bq/kg)	^{40}K Activity (Bq/kg)
Capacitors	[33.603, 43.654]	[48.588, 65.105]	[.297, 43.636]
Circuitboard	[0, 14.950]	[6.769, 42.484]	[0, 103.161]
Connectors	[0, 90.218]	[0, 107.727]	[0, 258.673]
BeCu Block	[0, 7.919]	[0, 14.412]	[0, 141.567]
Tungsten Block	[2.617, 2.939]	[0.332, 0.735]	[2.263, 3.718]
OFHC Copper	[0, 3.022]	[0, 3.032]	[0, 3.252]
Gasket Flanges	[0, 7.570]	[0, 21.139]	[0, 65.344]

These results, while potentially useful, are hurt by the high background surrounding the detector. To improve the sensitivity of these experiments, it would be useful to rebuild the shielding around the detector with an innermost layer of OFHC copper, or something similarly clean, to reduce the background due to impurities in the lead shielding. The sensitivity could also be improved by using more massive samples, and by measuring the samples for longer periods of time.

ACKNOWLEDGMENTS

Thank you to Jason Detwiler, Jonathan Leon, Julieta Gruszko, Clara Cuesta, Ian Guinn, Micah Buuck, Laura Bodine, and Alejandro Garcia at CENPA for their help and generosity with their time, as well as Mark Howe at the University of North Carolina for his help with ORCA. Thank you to the UW REU and the National Science Foundation for allowing me to do this research.

- [1] N. Abgrall et al., *Advances in High Energy Physics* **2014**, 365432 (2014).
- [2] Canberra Industries, "Reverse electrode coaxial ge detectors product sheet,".
- [3] G. Feldman and R. Cousins, *Physical Review D* **57**, 3873 (1998).

- [4] J. H. Hubbell and S. M. Seltzer, "Tables of x-ray mass attenuation coefficients and mass energy-absorption coefficients from 1 kev to 20 mev for elements $z = 1$ to 92 and 48 additional substances of dosimetric interest," (1996).